

## LOW-TEMPERATURE TRANSPORT PROPERTIES OF THE $\epsilon$ -PHASES Al-Pd-(Mn, Fe, Co, Rh)

### NIZKOTEMPERATURNE TRANSPORTNE LASTNOSTI $\epsilon$ -FAZ Al-Pd-(Mn, Fe, Co, Rh, ...)

Denis Stanić<sup>1</sup>, Igor Smiljanić<sup>1</sup>, Neven Barišić<sup>1</sup>, Janez Dolinšek<sup>2</sup>, Ante Bilušić<sup>1,3</sup>,  
Jagoda Lukatela<sup>1</sup>, Boran Leontić<sup>1</sup>, Ana Smontara<sup>1</sup>

<sup>1</sup>Institute of Physics, Bijenička 46, HR-1000 Zagreb, Croatia

<sup>2</sup>J. Stefan Institute, Jamova 39, SI-1000 Ljubljana, Slovenia

<sup>3</sup>Faculty of Natural Sciences, University of Split, N. Tesle 12, HR-21000 Split, Croatia  
dstanic@ifs.hr

Prejem rokopisa – received: 2007-07-12; sprejem za objavo – accepted for publication: 2007-12-14

We report results on low-temperature investigations of the electrical and thermal conductivity of the  $\epsilon$ -phases in the Al-Pd-Fe, Al-Pd-Co and Al-Pd-Rh systems, which are characterized by giant unit cells with a quasicrystals-like cluster substructure. The electrical resistivity is of the order of 100  $\mu\Omega$  cm and shows a weak temperature dependence in the investigated temperature interval 4–300 K. An interesting feature of the  $\epsilon$ -phases is their low thermal conductivity, which at room temperature is comparable to that of thermally insulating amorphous  $\text{SiO}_2$  and  $\text{Zr/YO}_2$  ceramics. While  $\text{SiO}_2$  and  $\text{Zr/YO}_2$  are also electrical insulators,  $\epsilon$ -phases exhibit an electrical conductivity typical of metallic alloys and offer an interesting combination of an electrical conductor and a thermal insulator. The reason for the weak thermal conductivity of the  $\epsilon$ -phases appears to be structural: large and heavy atomic clusters of icosahedral symmetry in the giant unit cell prevent the propagation of extended phonons and the lattice can no more efficiently participate in the heat transport.

Keywords: complex intermetallic alloys; physical properties, resistivity, thermal conductivity

Predstavljamo nizkotemperaturne raziskave električne in toplotne prevodnosti  $\epsilon$ -faz v sistemih Al-Pd-Fe, Al-Pd-Co in Al-Pd-Rh, ki jih karakterizirajo velike celice s podstrukturo iz klasterjev kvazikristalov. Električna upornost je reda velikosti 100  $\mu\Omega$  cm in je malo odvisna od temperature v preiskanem intervalu 4–300 K. Zanimiva značilnost  $\epsilon$ -faz je njihova majhna toplotna prevodnost, ki je pri sobni temperaturi primerljiva tisti pri toplotnih izolatorjih amorfnega  $\text{SiO}_2$  in  $\text{Zr/YO}_2$ -keramiki, ki pa sta električna izolatorja. Nasprotno,  $\epsilon$ -faze imajo električno prevodnost, ki je značilna za kovinske zlitine in dajejo zanimivo kombinacijo električnega prevodnika in toplotnega izolatorja. Vzrok za majhno toplotno prevodnost  $\epsilon$  faz so verjetno strukturni, veliki in težki klasterji atomov z ikosaedrično simetrijo, ki v veliki celici preprečujejo propagacijo razširjenih fononov, zato mreža ne more sodelovati učinkovito pri transportu toplote.

Ključne besede: kompleksne intermetalne zlitine, fizikalne lastnosti, upornost, toplotna prevodnost

## 1 INTRODUCTION

Among the complex metallic alloys (CMAs), an interesting family of related structures is found in the Al-Pd<sup>1</sup> and Al-Rh<sup>2</sup> alloys systems and their ternaries Al-Pd-(Mn, Fe, Co, Rh, etc.) with transition metals<sup>3–8</sup>. These so-called  $\epsilon$ -phases have been observed in wide compositional ranges and, depending on their composition, contain a row of giant-unit-cell orthorhombic structures and aperiodic structures in one dimension<sup>7</sup>. In the recent studies of Al-Pd-Fe<sup>5</sup>, Al-Pd-Co<sup>6</sup> and Al-Pd-Rh<sup>8</sup> phase diagrams, the concentration ranges of the  $\epsilon$ -phases were determined for different temperatures and large samples were grown. Here we present a study of their electrical and thermal properties and show that  $\epsilon$ -phases offer a promising combination of a metallic electrical conductor with a thermal insulator. In our recent investigation<sup>9</sup>, the physical properties of  $\epsilon$ -phases were determined in  $\text{Al}_{74}\text{Pd}_{22}\text{Mn}_4$ . The present work extends the exploration of these properties to a wide assortment of components, compositions and structural variants of the  $\epsilon$ -phases.

## 2 EXPERIMENTAL

The Al-Pd-Fe, Al-Pd-Co and Al-Pd-Rh samples investigated were polycrystalline materials, produced by levitation induction melting in a water-cooled copper crucible, as described in detail elsewhere<sup>5,6,8</sup>. Parts of the ingots were annealed under argon or vacuum for up to 2441 h and then water-quenched. The structural characterization was performed by powder X-ray diffraction and scanning electron microscopy, which showed that the selected samples were pure materials, not contaminated by secondary phases. Four Al-Pd-Fe, two Al-Pd-Co, two Al-Pd-Rh and an Al-Rh sample were included in the study. Their nominal compositions and electrical resistivity data ( $\rho_{300\text{ K}}$  and the ratio  $(\rho_{300\text{ K}}/\rho_{4\text{ K}})$ ) are given in **Table 1**. In the following we abbreviate their compositions by the symbols of their constituent elements and the number denoting the concentration (in %) of the transition element (e. g., the sample  $\text{Al}_{74}\text{Pd}_{12.5}\text{Co}_{13.5}$  is abbreviated as  $\text{AlPdCo}_{13.5}$ ).

In order to measure the electrical and thermal conductivity of a given material, a specimen in the form

**Table 1:** The nominal composition and the electrical resistivity data for the investigated samples**Tabela 1:** Nazivna sestava in podatki o električni upornosti preiskanih vzorcev

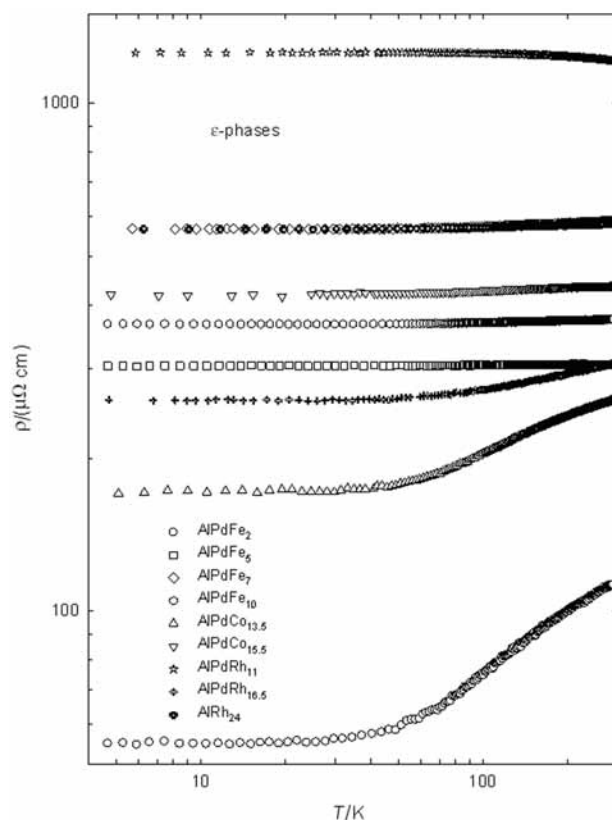
| Number | Composition  | Abbre-viation          | $\rho_{300\text{K}}/\mu\Omega\text{ cm}$ | $\rho_{300\text{K}}/\rho_{4\text{K}}$ |
|--------|--|------------------------|--|---------------------------------------|
| 1      | Al <sub>73</sub> Pd <sub>25</sub> Fe <sub>2</sub>      | AlPdFe <sub>2</sub>    | 112                                      | 2,02                                  |
| 2      | Al <sub>71</sub> Pd <sub>24</sub> Fe <sub>5</sub>      | AlPdFe <sub>5</sub>    | 270                                      | 1,18                                  |
| 3      | Al <sub>73</sub> Pd <sub>20</sub> Fe <sub>7</sub>      | AlPdFe <sub>7</sub>    | 586                                      | 1,03                                  |
| 4      | Al <sub>75,5</sub> Pd <sub>14,5</sub> Fe <sub>10</sub> | AlPdFe <sub>10</sub>   | 376                                      | 1,02                                  |
| 5      | Al <sub>74</sub> Pd <sub>12,5</sub> Co <sub>13,5</sub> | AlPdCo <sub>13,5</sub> | 260                                      | 1,52                                  |
| 6      | Al <sub>73,5</sub> Pd <sub>11</sub> Co <sub>15,5</sub> | AlPdCo <sub>15,5</sub> | 438                                      | 1,04                                  |
| 7      | Al <sub>74</sub> Pd <sub>15</sub> Rh <sub>11</sub>     | AlPdRh <sub>11</sub>   | 579                                      | 1,02                                  |
| 8      | Al <sub>74,5</sub> Pd <sub>9</sub> Rh <sub>16,5</sub>  | AlPdRh <sub>16,5</sub> | 308                                      | 1,19                                  |
| 9      | Al <sub>76</sub> Rh <sub>24</sub>                      | AlRh <sub>24</sub>     | 1212                                     | 0,97                                  |

of a bar with dimensions  $\approx (1.9 \times 0.5 \times 0.5)$  mm was cut from the ingot. The sample faces were then polished using emery paper. The sample was cooled using a <sup>4</sup>He flux cryostat between 4 K and 300 K. The electrical resistivity was measured by a four-probe low-frequency ac-method, whereas for the measurement of the thermal conductivity a standard steady-state heat-flow technique was used. For thermal conductivity measurements, one end the bar-shaped sample was glued to a heat sink made of copper by means of GE varnish. The sample heater, attached to the other end with the same glue, consisted of a 100-V ruthenium-oxide chip resistor. With the aim to measure the thermal gradient along the sample we used calibrated chromel-gold/iron thermocouples. Very thin, 25  $\mu\text{m}$  in diameter, and up to 10 cm long, wires were chosen in order to reduce the heat flow through the thermocouples. The temperature difference of the sample was always kept smaller than 1 K. The cooling (heating) rate was generally 5 K/h or less. Thermal conductivity measurements of materials with low thermal conductivity values are generally difficult to perform at high temperatures because of the detrimental effect of radiative losses on the results. In order to limit this type of energy dissipation, a cylindrical radiation shield in good thermal contact with the heat sink was used. With this setup, the radiative losses in our measurements were estimated to be below 1 % of the applied power over the whole temperature range and the relative accuracy of the measurement (1–2 %) was much better than that for the absolute values. Considering the length of the samples and the lateral extension of the thermal contacts, the uncertainty in the geometrical factor was estimated to be about 10–20 %, where the larger errors correspond to the shorter samples. We used the same sample geometry for both the electrical resistivity and thermal conductivity measurements in order to avoid additional uncertainties that could arise in the subtraction of the electronic contribution to the measured thermal conductivity.

### 3 RESULTS AND ANALYSIS

#### 3.1 Electrical resistivity

The resistivity of all the samples is shown in **Figure 1**. The room temperature resistivity of most samples is in the range 200–600  $\mu\Omega\text{ cm}$  and exhibits small temperature variations of a few percentages between 300 K and 4 K. Exceptions are the samples AlPdFe<sub>2</sub>, with lower resistivities ( $\rho_{300\text{K}} = 112 \mu\Omega\text{ cm}$  and  $\rho_{300\text{K}}/\rho_{4\text{K}} = 2.02$ ), and AlRh<sub>24</sub>, with the highest resistivity ( $\rho_{300\text{K}} = 1212 \mu\Omega\text{ cm}$ ). The AlRh<sub>24</sub> sample also exhibits a small negative temperature coefficient ( $\rho_{300\text{K}}/\rho_{4\text{K}} = 0.97$ ), in contrast to all the other samples, which show positive temperature coefficients. The above resistivity (of polygrain samples) compares well to the resistivity of monocrystalline  $\varepsilon$ -phase Al–Pd–Mn, which amounts to  $\rho_{300\text{K}} \approx 200 \mu\Omega\text{ cm}$ <sup>9</sup> and exhibits a practically zero temperature coefficient ( $\rho_{300\text{K}}/\rho_{4\text{K}} \approx 1.01$ ). An interesting feature, related to the weak Curie paramagnetism detected recently in the samples<sup>10</sup>, is also observed in the  $\rho(T)$  curves. In **Figure 2**, we show the resistivity of the three Al–Pd–Fe samples with the highest Fe content (i.e. AlPdFe<sub>10</sub>, AlPdFe<sub>7</sub> and AlPdFe<sub>5</sub>) on a  $\rho/\rho_{300\text{K}}$  normalized scale. The resistivity exhibits a small, positive temperature coefficient, indicating that phonons play a role in the temperature dependence of  $\rho(T)$ . At

**Figure 1:** The electrical resistivity  $\rho(T)$  of the  $\varepsilon$ -phase samples in the Al–Pd–Fe, Al–Pd–Co and Al–Pd–Rh systems**Slika 1:** Električna prevodnost  $\rho(T)$  za  $\varepsilon$  faze v sistemih Al–Pd–Fe, Al–Pd–Co in Al–Pd–Rh

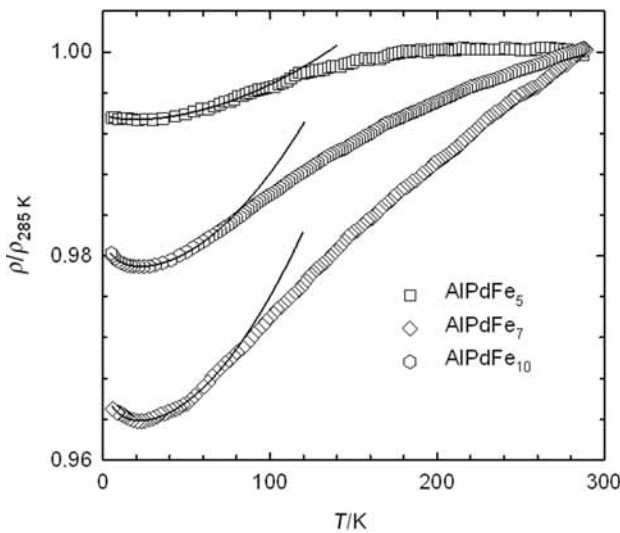


**Figure 2:** The electrical resistivity of the three Al-Pd-Fe samples with the highest Fe content on a  $\rho/\rho_{300}$  K normalized scale.

**Slika 2:** Električna upornost treh vzorcev Al-Pd-Fe z največjo vsebnostjo Fe na  $\rho/\rho_{300}$  normalizirani skali

low temperatures, the resistivity exhibits a minimum that is most pronounced for the AlPdFe<sub>10</sub> sample. It is still clearly recognizable for the AlPdFe<sub>7</sub> and becomes less obvious for the AlPdFe<sub>5</sub>. According to magnetic measurements <sup>10</sup>, it is reasonable to assume that Al-Pd-Fe samples with a higher Fe content are more magnetic. For the AlPdFe<sub>5</sub> sample it was estimated that a fraction of 0.00041 of all the Fe atoms in the sample carry localized magnetic moments <sup>10</sup>. It is known that a small amount of transition-metal impurities of this order of magnitude dissolved in a metal introduce a minimum in the  $\rho(T)$  (e.g., in Cu metal with 0.00044 Fe, the minimum was observed at 25 K <sup>12</sup>). The reason is the s-d exchange interaction between the s-moments of the conduction electrons and the d-moments of the transition-metal impurities, which contributes to the resistivity <sup>11</sup>. The total resistivity at low temperatures can be expressed as a sum of the electron-phonon contribution (e.g., by the Bloch-Grüneisen contribution  $\rho = \rho_0 + bT^5$  for regular metals, or by its modification  $\rho = \rho_0 + bT^2$  in the case of amorphous alloys <sup>13</sup>, to which  $\epsilon$ -phases show certain resemblance on the interatomic scale due to an icosahedral near-neighbor coordination that is characteristic of the amorphous alloys as well <sup>14</sup>) and the s-d contribution:

$$\rho = a + bT^2 + d \lg T \quad (1)$$

where  $a$ ,  $b$  and  $d$  are fitting parameters. Using this expression, one can fit well the experimental data up to 70 K, but fits should be considered as qualitative due to the limited temperature range of the analysis. The shift of the resistivity minimum to lower temperatures for samples with a lower Fe concentration is consistently observed, in agreement with the prediction of the expression.

Also of general interest, in the context of giant-unit-cell complex metallic alloys, is the question which of the two coexisting physical length scales – the large-scale periodicity versus the atomic-scale icosahedral order – plays the dominant role in determining the electrical transport properties of the complex metallic alloys. This question can be addressed by applying pressure to the sample in an electrical resistivity experiment. Pressure-induced compression of the lattice brings the atoms closer together, so that the overlap of the atomic potentials is larger and the potential barriers between neighboring atoms are reduced, which should enhance the electronic transport. The application of pressure should thus change the electrical resistivity due to atomic-scale effects. Indeed, preliminary measurements show that the resistivity of  $\epsilon$ -Al<sub>75</sub>Pd<sub>20</sub>Fe<sub>5</sub> drops significantly with pressure from  $\rho_{300}$  K (0 bar) = 306  $\mu\Omega$  cm to  $\rho_{300}$  K (17.8 kbar) = 284  $\mu\Omega$  cm, thus by 7 % relative to the  $p = 0$  value, whereas this reduction amounts 8.5 % at 4 K <sup>10</sup>. This behavior is consistent with the consideration that the resistivity of a complex metallic material is governed by the smaller of the two coexisting physical length scales – that of the interatomic distances – whereas the large-scale periodicity is of marginal importance for the electronic transport.

### 3.2 Thermal conductivity

The measured thermal conductivities  $\kappa(T)$  of all the samples are displayed in **Figure 3** on a lg-lg scale. The surprising results are the low  $\kappa(T)$  values, which are in the range  $\kappa_{300}$  K  $\approx$  2–10 W/mK at room temperature. The conductivities of the AlRh<sub>24</sub> and AlPdRh<sub>11</sub> samples are even as low as  $\kappa_{300}$  K = 2 W/mK. These  $\kappa_{300}$  K values, very low for alloys of regular metals, are comparable to the thermal conductivity of amorphous SiO<sub>2</sub> ( $\kappa_{300}$  K = 2.8 W/mK), a known electrical and thermal insulator, as well as to the technologically widespread thermally insulating material yttrium-doped zirconia ceramics Zr<sub>1-x</sub>Y<sub>x</sub>O<sub>2-x/2</sub> ( $x < 0.2$ ), where  $\kappa_{300}$  K  $\approx$  2 W/mK <sup>21</sup>. The thermal conductivity model appropriate to complex metallic alloys with the large-scale periodicity of the lattice and the small-scale atomic clustering structure has been described in detail in the previous investigation of  $\epsilon$ -phases in the Al-Pd-Mn system <sup>9</sup> as well as of the giant-unit-cell orthorhombic phases in the Al-Cr-Fe system <sup>15</sup> and the "Bergman phase" Mg<sub>32</sub>(Al,Zn)<sub>49</sub> <sup>16</sup>. The total thermal conductivity parameter  $\kappa(T)$  is divided into three terms:

$$\kappa(T) = \kappa_{el}(T) + \kappa_D(T) + \kappa_H(T) \quad (2)$$

The electronic contribution  $\kappa_{el}$  is estimated from the measured electrical resistivity data using the Wiedemann-Franz law,  $\kappa_{el} = L_0 T / \rho$ , where  $L_0$  is the Lorenz number. The lattice contribution  $\kappa_l = \kappa - \kappa_{el}$  is analysed by considering the propagation of long-wavelength phonons within the Debye model and the hopping of localized vibrations. This picture assumes that large

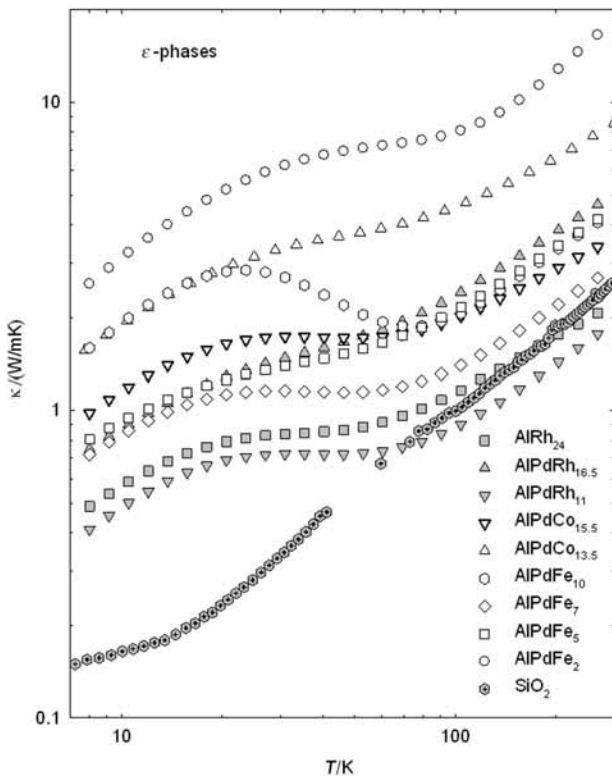


**Figure 3:** The thermal conductivities  $\kappa(T)$  of the  $\varepsilon$ -phase samples between 8 K and 300 K. The thermal conductivity of amorphous  $\text{SiO}_2$  is shown for comparison.

**Slika 3:** Toplotna prevodnost  $\kappa(T)$  vzorcev  $\varepsilon$ -faz med 8 K in 300 K. Toplotna prevodnost amorfnega  $\text{SiO}_2$  je prikazana za primerjavo

atomic clusters of icosahedral symmetry strongly suppress the propagation of phonons in the lattice of complex metallic alloys. The exceptions are long-wavelength acoustic phonons, for which this material is an elastic continuum, and fracton-like localized vibrations within the cluster substructure that can participate in the heat transfer via thermally activated hopping. In the simplest model, the hopping of localized vibrations is described by a single activation energy  $E_a$ , yielding a contribution to the thermal conductivity  $\kappa_H = \kappa_H^0 \exp(-E_a/k_B T)$ , where  $\kappa_H^0$  is a constant. The Debye thermal conductivity is written as:

$$\kappa_D = C_D T^3 \int_0^{\theta_D/T} \tau(x) \frac{x^4 e^x}{(e^x - 1)^2} dx \quad (3)$$

where  $C_D = k_B^4 / 2\pi^2 \bar{v} \hbar^3$ ,  $\bar{v}$  is the average sound velocity,  $\theta_D$  is the Debye temperature,  $\tau$  is the phonon relaxation time and  $x = \hbar\omega/k_B T$ , where  $\hbar\omega$  is the phonon energy. The different phonon-scattering processes are incorporated into the relaxation time  $\tau(x)$  and we assume that Matthiessen's rule is valid,  $\tau^{-1} = \sum \tau_j^{-1}$ , where  $\tau_j^{-1}$  is a scattering rate related to the  $j$ -th scattering channel. In analogy to the  $\varepsilon$ -phases in Al-Pd-Mn<sup>9</sup>, we consider two dominant scattering processes in the investigated temperature interval (from 8 K to 300 K): (1) the scattering of phonons on structural defects of the

stacking-fault type with the scattering rate  $\tau_{sf}^{-1} = Ax^2 T^2$  and (2) umklapp processes with the phenomenological form of the scattering rate pertinent to complex metallic alloys<sup>9,15</sup>,  $\tau_{um}^{-1} = Bx^\alpha T^\beta$ , so that  $\tau^{-1} = \tau_{sf}^{-1} + \tau_{um}^{-1}$ . The Debye temperature of the investigated  $\varepsilon$ -phases is not known, therefore we have used the  $\theta_D$  value reported for the related icosahedral *i*-Al-Pd-Mn quasicrystals, where  $\theta_D$  was commonly found to be close to 500 K<sup>18,19</sup>. Since our  $\kappa(T)$  data are available only up to 300 K, it turns out that the fit is insensitive to a slight change of this  $\theta_D$  value, so that a fixed  $\theta_D = 500$  K is used. The Debye constant  $C_D$  was also not taken as a free

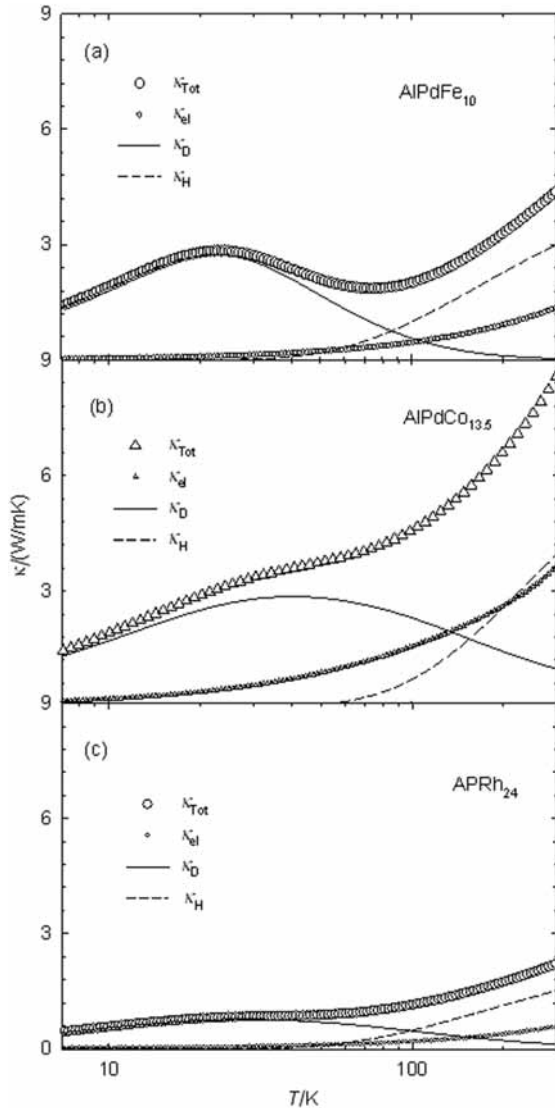


**Figure 4:** Thermal conductivities  $\kappa(T)$  of the AlPdFe<sub>10</sub> (a), AlPdCo<sub>13.5</sub> (b) and AlPdRh<sub>24</sub> (c). The three contributions to the total  $\kappa(T)$  – large symbols, obtained using Eq. (2) are shown separately. The electronic contribution  $\kappa_{el}$  – small symbols, the Debye contribution  $\kappa_D$  – solid line and the hopping contribution  $\kappa_H$  – dashed line.

**Slika 4:** Toplotne prevodnosti  $\kappa(T)$  za AlPdFe<sub>10</sub> (a), AlPdCo<sub>13</sub> (b) in AlPdRh<sub>24</sub> (c). Trije deli celotne  $\kappa(T)$  – veliki simboli, dobljeni z uporabo enačbe (2), so prikazani ločeno. Elektronski delež  $\kappa_{el}$  – majhni simboli, Debyev delež  $\kappa_D$  – cela črta in hopping delež  $\kappa_H$  – črtkana črta.

**Table 2:** Fit parameters of the thermal conductivities  $\kappa(T)$  from **Figure 3****Tabela 2:** "Fit"-parametri za topotno prevodnost  $\kappa(T)$  iz slike 3

| Sample                 | $A \times 10^6$<br>$s^{-1} K^{-2}$ | $B \times 10^3$<br>$s^{-1}$ | $\alpha$ | $\beta$ | $\kappa_h^o$<br>(W/mK) | $E_a$ (K) |
|------------------------|------------------------------------|-----------------------------|----------|---------|------------------------|-----------|
| AlPdFe <sub>2</sub>    | 4.2                                | 1.5                         | 2.0      | 3.6     | 37.2                   | 373       |
| AlPdFe <sub>5</sub>    | 11.3                               | 11.4                        | 2.2      | 3.5     | 3.0                    | 215       |
| AlPdFe <sub>7</sub>    | 12.5                               | 5.2                         | 1.3      | 3.9     | 2.8                    | 174       |
| AlPdFe <sub>10</sub>   | 6.3                                | 0.14                        | 1.6      | 4.6     | 5.2                    | 166       |
| AlPdCo <sub>13.5</sub> | 6.1                                | 2.9                         | 2.5      | 3.6     | 9.4                    | 259       |
| AlPdCo <sub>15.5</sub> | 9.4                                | 3.7                         | 2.0      | 3.8     | 5.0                    | 183       |
| AlPdRh <sub>11</sub>   | 24.6                               | 38.1                        | 2.4      | 4.0     | 1.0                    | 176       |
| AlPdRh <sub>16.5</sub> | 12.0                               | 18.3                        | 2.1      | 3.4     | 4.7                    | 238       |
| AlRh <sub>24</sub>     | 18.4                               | 11.0                        | 2.0      | 3.7     | 2.7                    | 171       |

parameter, but was instead calculated by using  $\bar{v} = 4\,004$  ms<sup>-1</sup>, a value determined for the *i*-Al-Pd-Mn from ultrasonic data<sup>20</sup>. The thermal conductivities of the  $\epsilon$ -phase samples were analysed by means of **Eq. (2)**. The total  $\kappa(T)$ 's were resolved into the electronic ( $\kappa_{el}$ ), Debye ( $\kappa_D$ ) and hopping ( $\kappa_H$ ) contributions, which are shown separately on the graphs. The  $\kappa(T)$ 's of the Al-Pd-Fe sample are shown in **Figure 4a**, that of Al-Pd-Co in **Figure 4b**, and that of Al-Pd-Rh in **Figure 4c**, whereas the fit parameters are collected in **Table 2**, together with the fit parameters obtained for all the investigated samples. A common characteristic of all the  $\epsilon$ -phase samples is a small Debye contribution (its maximum value is in the range  $\kappa_{D,max} \approx 0.5\text{--}4$  W/mK) and a significant hopping contribution at elevated temperatures. A qualitative explanation of this result is that large atomic clusters of icosahedral symmetry suppress the heat transfer by phonons, whereas localized cluster vibrations still provide a weak lattice heat-conduction channel. In addition, conduction electrons contribute the usual channel to the heat conductivity, but since the electrical resistivity of the  $\epsilon$ -phase is of few 100  $\mu\Omega$  cm, the electronic thermal conductivity contribution is also not large. Consequently, the total thermal conductivities of the  $\epsilon$ -phase materials are about the same as that of amorphous SiO<sub>2</sub>. Here it is important to point out that while SiO<sub>2</sub> is both a thermal and an electrical insulator, the  $\epsilon$ -phase complex metallic alloys offer a combination of a thermal insulator with an electrical conductor, which can be considered as a "smart" property of the material, not realized in conventional solid-state materials. Here we also stress that our thermal conductivity values, obtained on polygrain materials, are practically the same as those obtained on  $\epsilon$ -phase Al-Pd-Mn monocrystalline samples<sup>9</sup>. Thus, polycrystallinity does not have a significant influence on the thermal response of the  $\epsilon$ -phase material. The cluster substructure very likely already provides enough phonon scattering centers to suppress the phonon propagation, so that additional scattering at the grain boundaries does not

add much to this effect. A similar consideration also seems to hold for the electron scattering in the electronic transport. The thermal conductivity fit parameters in **Table 2** allow us to derive some average properties of the  $\epsilon$ -phases. The average hopping activation energy of the localized vibrations is  $\bar{E}_a = 209 \pm 49$  K (or  $(18 \pm 4)$  meV), which is similar to the values observed in *i*-Al-Pd-Mn QC's<sup>9</sup>. The average values of the exponents  $\alpha$  and  $\beta$  that govern the frequency and temperature dependencies of the *umklapp* rate are  $\bar{\alpha} = 2.0 \pm 0.4$  and  $\bar{\beta} = 3.8 \pm 0.8$ , yielding the average dependence  $\tau_{um}^{-1} \propto \omega^2 T^{1.8}$ . This is close to the phenomenological power-law  $\omega^2 T^2$ , sometimes observed in systems with a dense distribution of energy gaps in the vibrational spectrum, like in icosahedral Al-based quasicrystals. Very small thermal conductivities,  $\kappa < 4.5$  W/mK in the temperature interval 2–300 K, were reported recently<sup>27</sup> also for a series of related complex metallic materials, the Al-based Mackay-type 1/1 cubic approximants. In contrast to our phenomenological analysis of the thermal conductivity, the explanation of the anomalously low thermal conductivity in<sup>28</sup> was derived from first-principle calculations of the phonon dispersion, using crystallographic structure data of the investigated materials. It was found that the combination of a small group velocity and the large number of optical phonon branches caused by the large number of atoms in the unit cell greatly reduces the lattice thermal conductivity by increasing the probability of the *umklapp* processes in the phonon scattering. The presence of vacancies in the structure further enhances this tendency. We expect that a similar microscopic picture also explains the anomalously low thermal conductivity of the  $\epsilon$ -phases. There is one marked difference in the thermal conductivities of the  $\epsilon$ -phases and the approximants studied in<sup>28</sup>. While the thermal conductivities of the latter materials exhibit a very weak temperature dependence above 100 K (see **Figure 2** of<sup>28</sup>), our  $\epsilon$ -phase materials exhibit an exponential increase above about 70 K (**Figure 4**), which we model phenomenologically with a thermally activated behavior using an activation energy  $E_a$  and attribute it to the hopping of localized vibrations (i.e., a given locally-vibrating atomic cluster "hits" its neighbor).

#### 4 CONCLUSIONS

The electrical resistivity of the  $\epsilon$ -phases is moderate, in the range of a few 100  $\mu\Omega$  cm, and shows a weak temperature dependence (in most cases of a few percentages) in the investigated temperature interval 4–300 K. An interesting feature of the  $\epsilon$ -phases is their low thermal conductivity, which at room temperature is about the same as that of known thermal insulators like amorphous SiO<sub>2</sub> and Zr/YO<sub>2</sub> ceramics. While SiO<sub>2</sub> and Zr/YO<sub>2</sub> are also electrical insulators, the  $\epsilon$ -phases exhibit an electrical conductivity typical of metallic alloys, so

that this material offers an interesting combination of an electrical conductor together with a thermal insulator. The reason for the weak heat conductivity of the  $\epsilon$ -phases appears to be structural: large and heavy atomic clusters of icosahedral symmetry in the giant unit cell suppress the propagation of extended phonons, so that the lattice cannot efficiently participate in the heat transport (apart from the remaining weak channel of the hopping of localized vibrations). As the cluster substructure is a common feature of complex metallic alloys, a low thermal conductivity at a moderate electrical conductivity can be expected to be a general property of this class of materials. The  $\epsilon$ -phase material can thus be considered as a promising candidate for the development of a technologically interesting "smart" material that combines the properties of an electrical conductor with a thermal insulator.

### Acknowledgements

We would like to thank Mr. B. Grushko for giving us the samples and for stimulating discussions. This work was done within the activities of the EU Network of Excellence "Complex Metallic Alloys" (Contract No. NMP3-CT-2005-500140), and has been supported in part by the Ministry of Science, Education and Sports of Republic of Croatia through the Research Projects No. 035-0352826-2848 and 177-0352828-0478.

### 5 REFERENCES

- <sup>1</sup> M. Yurechko, A. Fattah, T. Velikanova, B. Grushko, *J. Alloys Compd.* 329 (**2001**), 173–181
- <sup>2</sup> B. Grushko, J. Gwóźdż, M. Yurechko, *J. Alloys Compd.* 305 (**2000**), 219–224
- <sup>3</sup> M. Boudard, H. Klein, M. de Boissieu, M. Audier, H. Vincent, *Philos. Mag. A* 74 (**1996**), 939–956
- <sup>4</sup> H. Klein, M. Audier, M. Boudard, M. de Boissieu, L. Beraha and M. Duneau, *Philos. Mag. A* 73 (**1996**), 309–331
- <sup>5</sup> S. Balanetskyy, B. Grushko, T.Ya. Velikanova, K. Urban, *J. Alloys Compd.* 376 (**2004**), 158–164
- <sup>6</sup> M. Yurechko, B. Grushko, T. Velikanova, K. Urban, *J. Alloys Compd.* 337 (**2002**), 172–181
- <sup>7</sup> S. Balanetskyy, B. Grushko, T. Ya. Velikanova, Z. Kristall. 219 (**2004**), 548–553
- <sup>8</sup> B. Przeździński, B. Grushko, M. Surowiec, *Intermetallics* 14 (**2006**), 498–504
- <sup>9</sup> J. Dolinšek, P. Jeglič, P. J. McGuiness, Z. Jagličić, A. Bilušić, Ž. Bihar, A. Smontara, C. V. Landrau, M. Feuerbacher, B. Grushko, K. Urban, *Phys. Rev. B* 72 (**2005**), 064208-1–11
- <sup>10</sup> A. Smontara, I. Smiljanić, A. Bilušić, B. Grushko, S. Balanetskyy, Z. Jagličić, S. Vrtnik, J. Dolinšek, *J. Alloys Compd.* 450 (**2008**) 92–102
- <sup>11</sup> See, e.g.: U. Mizutani, *Electron Theory of Metals*, Cambridge University Press (2001), p. 416
- <sup>12</sup> J. M. Ziman, *Electrons and Phonons*, Clarendon Press, Oxford (1962), 244
- <sup>13</sup> U. Mizutani, *Electron Theory of Metals*, Cambridge University Press (2001), 480
- <sup>14</sup> W. K. Luo, H. W. Sheng, F. M. Alamgir, J. M. Bai, J. H. He, E. Ma, *Phys. Rev. Lett.* 92 (**2004**), 145502–145505
- <sup>15</sup> Ž. Bihar, A. Bilušić, J. Lukatela, A. Smontara, P. Jeglič, P. J. McGuiness, J. Dolinšek, Z. Jagličić, J. Janovec, V. Demange, J. M. Dubois, *J. Alloys Compd.* 407 (**2006**), 65–73
- <sup>16</sup> A. Smontara, I. Smiljanić, A. Bilušić, Z. Jagličić, M. Klanjšek, S. Roitsch, J. Dolinšek, M. Feuerbacher, *J. Alloys Compd.* 439 (**2007**), 29–38
- <sup>17</sup> R. Berman, *Thermal Conduction in Solids*, Oxford University Press (1978), 23
- <sup>18</sup> A. Bilušić, A. Smontara, J. Dolinšek, P.J. McGuiness, H.R. Ott, *J. Alloys Compd.* 432 (**2007**), 1–6
- <sup>19</sup> C. Wälti, E. Felder, M. A. Chernikov, H. R. Ott, M. de Boissieu, C. Janot, *Phys. Rev. B* 57 (**1998**), 10504–10511
- <sup>20</sup> Y. Amazit, M. de Boissieu, A. Zarembowitch, *Europhys. Lett.* 20 (**1992**), 703–706
- <sup>21</sup> R. Mévrel, J.-C. Laizet, A. Azzopardi, B. Leclercq, M. Poulain, O. Lavigne, D. Demange, *J. Eur. Ceram. Soc.* 24 (**2004**), 3081–3089
- <sup>22</sup> C. Janot, A. Magerl, B. Frick, M. de Boissieu, *Phys. Rev. Lett.* 71 (**1993**), 871–874
- <sup>23</sup> M. de Boissieu, M. Boudard, R. Bellissent, M. Quilichini, B. Henion, R. Currat, A.I. Goldman, C. Janot, *J. Phys.: Condens. Matter.* 5 (**1993**), 4945–4966
- <sup>24</sup> M. Boudard, M. de Boissieu, S. Kycia, A. I. Goldman, B. Hennion, R. Bellissent, M. Quilichini, R. Currat, C. Janot, *J. Phys.: Condens. Matter.* 7 (**1995**), 7299–7308
- <sup>25</sup> M. Krisch, R. A. Brand, M.A. Chernikov, H. R. Ott, *Phys. Rev. B* 65 (**2002**), 134201-1–8
- <sup>26</sup> T. Takeuchi, N. Nagasako, R. Asahi, U. Mizutani, *Phys. Rev. B* 74 (**2006**), 054206-1–12
- <sup>27</sup> N. F. Mott, H. A. Jones, *The Theory of the Properties of Metals and Alloys*, Clarendon, Oxford 1936, 23